Journal of Marine Science and Technology

Volume 23 | Issue 5 Article 11

EFFECTS OF THE SHEAR GAPS ON THE BREAKAGE BEHAVIOR OF SILTY SAND PARTICLE

Jing-Wen Chen
Department of Civil Engineering, National Cheng-Kung University, Tainan, Taiwan, R.O.C., geochen@mail.ncku.edu.tw

Bo-Rung Lin
Department of Civil Engineering, National Cheng-Kung University, Tainan, Taiwan, R.O.C.

Shun-Chieh Hsieh
Department of Land Management and Development, Chang Jung Christian University, Tainan, Taiwan, R.O.C.

Wei F. Lee
Ground Master Construction Co., Ltd., Taipei, Taiwan, R.O.C.

EFFECTS OF THE SHEAR GAPS ON THE BREAKAGE BEHAVIOR OF SILTY SAND PARTICLE

Acknowledgements

The authors would like to thank Prof. Kenji Ishihara, Prof. Takaji Kokusyo (CHUO University, Tokyo, Japan), and Prof. Yie-Ruey Chen (Chang Jung Christian University, Tainan, Taiwan) for their help and advice during instrument development and design and suggestions for the procedures of the test.

Journal of Marine Science and Technology, Vol. 23, No. 5, pp. 678-684 (2015)
DOI: 10.6119/JMST-015-0521-4

EFFECTS OF THE SHEAR GAPS ON THE BREAKAGE BEHAVIOR OF SILTY SAND PARTICLE

Jing-Wen Chen[1], Bo-Rung Lin[1], Shun-Chieh Hsieh[2], and Wei F. Lee[3]

Key words: direct shear test, shear gap, fines content, particle crushing.

ABSTRACT

To determine the breakage behavior of soil particles on a sliding surface, which is subjected to high overburden stress, modified direct shear tests were conducted on silty sand collected from Kaohsiung City, Taiwan. The sliding surfaces of the soil was simulated using different shear gaps of the shear box in the tests. The behavior of the particle breakage and strength properties of the sand were investigated. The results indicated that finer soil particles exhibited a lower breakage potential and breakage amount of sand particles, whereas a higher void ratio tended to lead to a higher breakage potential and breakage amount. For soil samples consisting of the same amount of fine particles, wider shear gaps caused a higher void ratio, whereas the increment of fines content and volumetric strain were both reduced after the shearing process.

I. INTRODUCTION

Particle breakage refers to the breakage of soil structure when soil particles are subjected to an external load and split into particles of equal or unequal sizes. Particle breakage can generally be divided into two forms: tensile failure caused by pressure or bending, and shear failure caused by shearing force.

Hardin (1985) indicated that the breakage characteristics of sand are mainly affected by its particle properties (particle size, particle shape, and hardness), particle composition (void ratio and gradation), and loading types (stress magnitude and stress path). Coarser particles are more likely to break during a load transmission compared with finer particles because of increased stress concentration phenomena at the contact surfaces caused by a smaller contact area between particles.

Lee and Seed (1967) and Miura et al. (1983) have discovered that water accelerated the particle breakage process, which was probably due to slight fissures that already existed on the particles or new fissures caused by excessive stress on the contact area. These fissures were expanded by water through capillarity, which accelerated soil particle breakage and decreased their strength because of the swollen volume.

The increase in percent passing a certain size after testing has often been used in previous studies as an indicator for measuring particle breakage. Among them, Leslie (1963) used the percent passing the sieve on which the original material was 100% retained. Marsal (1965) performed sieve analysis on some samples (e.g., sand, gravel, and crushed stone) before and after testing and defined the particle breakage amount (B_g) as the largest increase in particle amount retained on a certain sieve size before and after testing. Marsal stated that B_g increased as one-dimensional consolidation stress (σ_a) and axial stress at failure (σ_{1f}) increased in a triaxial test, but decreased as initial dry density increased. Marsal (1965) determined that it was due to the improvement of the interlocking effect caused by contact stresses between particles as force increased and initial dry density decreased. Subsequently, Leslie (1975) used the increase in percent passing the sieve on which 90% of the original sample was retained.

The breakage measure can be related to the particle size scale instead of the percent fine scale. Lee and Farhoomand (1967) conducted triaxial compression tests on decomposed granite soil samples with various particle size distributions under the same stress conditions and determined the ratio D_{15i}/D_{15a}, where D_{15i} is the diameter for which 15% of the original sample is finer, and D_{15a} is the diameter for which 15% of the loaded sample is finer.

Hardin (1985) defined the breakage potential (B_p) as the area between the line particle size $D = 0.074$ mm and the part of the particle size distribution curve for which D is larger than 0.074 mm. B_t is the total breakage, which is equal to the original breakage potential minus the breakage potential after loading. In addition, Hardin defined the relative breakage (B_r) as the ratio of the total breakage and breakage potential (i.e.,

Paper submitted 12/31/14; revised 03/13/15; accepted 05/21/15. Author for correspondence: Jing-Wen Chen (e-mail: geochen@mail.ncku.edu.tw).
[1] Department of Civil Engineering, National Cheng-Kung University, Tainan, Taiwan, R.O.C.
[2] Department of Land Management and Development, Chang Jung Christian University, Tainan, Taiwan, R.O.C.
[3] Ground Master Construction Co., Ltd., Taipei, Taiwan, R.O.C.

$B_r = B_t/B_p$). The total breakage B_t for a given soil can be expressed as a function of six variables accounting for the effects of particle size distribution, the state of effective stress and effective stress path, initial void ratio, particle shape, and particle hardness (Eq. (1)).

$$B_t = f(B_p,\ \tau,\ \sigma_0',\ e_0,\ n_s,\ h) \tag{1}$$

where B_p, τ, σ_0', e_0, n_s, and h represent the breakage potential, shear stresses, effective octahedral normal stresses, initial void ratio, particle shape, and particle hardness, respectively.

Hardin (1985) estimated the total breakage expected for a given soil subjected to a specified loading by using Eq. (2).

$$B_t = \frac{B_p S^{n_b}}{1+S^{n_b}} \tag{2}$$

where B_p is the breakage potential, and n_b and S are shown in Eq. (3) and Eq. (4), respectively.

$$n_b = \frac{h^2}{(1+e_0)n_s} + 0.3 \tag{3}$$

$$S = \frac{(1+e_0)n_s}{800\ h^2}\ \frac{\sigma_0'}{p_a}\left[1+9\left\{\frac{\tau_0}{\sigma_0'}\right\}^3\right] \tag{4}$$

The definitions of the symbols in this equation are the same as mentioned. P_a is atmospheric pressure.

Hardin (1985) used the findings of Lee and Farhoomand (1967) to analyze the breakage potential and total breakage and found a linear relationship between them, suggesting that changing the particle size distribution is unlikely to affect the relative breakage if test conditions remain unchanged.

Zhao et al. (2008) determined a linear relationship between sand particle breakage and plastic work when a direct shear test was performed under high pressure conditions. The effect of soil particle breakage was found to be the main cause of the nonlinear shear behavior. Zhang et al. (2009) learned from triaxial test results that the influences of particle breakage on the shear strength of soil increase as the confining pressure increases. When the breakage attains a certain level, the breaking process gradually weakens and its influences on soil strength tend to be stable.

In general, the mechanical behavior of low-plasticity silt shows a dualism between sand and clay. When soil is dominated by sand particles but simultaneously has a substantial amount of low-plasticity silt filling the void between the sand particles, or the sand particles are isolated by the silt, its engineering properties is inevitably affected by the finer particles. Therefore, soil samples containing low-plasticity silt were examined in this study to investigate the particle breakage characteristics and their effects on soil strength. A series of tests were then performed using a modified direct shear test apparatus at different shear gaps.

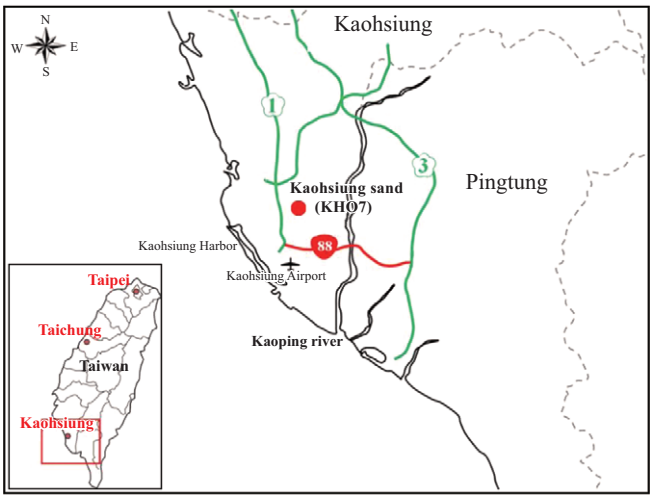

Fig. 1. Location of the Kaohsiung site.

II. TEST SAMPLES

According to Lee et al. (2012), soil layers in Southwestern Taiwan contain a high proportion of low-plasticity silt because of the influences of topography and climate in addition to the completion of weathering, transportation, and deposition process within a short period.

In this study, Kaohsiung sand (KH07) extracted from Southwestern Taiwan was used as the representative sample (Fig. 1). KH07 is gray silty sand (SP-SM) with a standard penetration test N-value between 11 and 18. The average moisture content in situ is approximately 28.1%, with a wet unit weight of 2.0 gf/cm^3. The dry unit weight is 1.56 gf/cm^3 with a liquid limit (*LL*) of 24.9 and a void ratio (e) of 0.712, and the sand is considered medium dense on site.

Fig. 2 presents the particle size distribution curves of an undisturbed sample extracted from a test pit along with those of remodeled samples after sieve and hydrometer analyses. The filled squares represent the results for the undisturbed sample, and the remainder represents the results for the remodeled samples with different fines contents. The curve of the undisturbed sample shows that KH07 is soil with a poor gradation. The remodeled samples with different fines contents (0%, 20%, and 40%) were produced in this study. The weight of soil required for the samples under different test conditions was calculated using the relative density test results (Table 1) and particle size distribution curves of the samples with different fines contents. The test results showed that the highest and lowest void ratios of the specimens tended to decrease as the fines content increased; however, this result was reversed after the fines content surpassed 30%. Therefore, the densest arrangement of low-plasticity silt particles in KH07 occurred when the fines content was 30%.

Table 1. Basic properties of the undisturbed and remodeled soil samples with different fines contents.

	Undisturbed sample	Remodeled samples		
FC (%)	12	0	20	40
G_s	2.67	2.71	2.65	2.70
$\gamma_{d,\max(\mathrm{gf/cm^3})}$	-	1.561	1.735	1.801
$\gamma_{d,\min(\mathrm{gf/cm^3})}$	-	1.199	1.254	1.262
$e_{\max}$	-	1.26	1.113	1.139
$e_{\min}$	-	0.736	0.527	0.499
D_{60} (mm)	0.22	0.21	0.2	0.16
D_{50} (mm)	0.19	0.18	0.18	0.11
D_{30} (mm)	0.13	0.12	0.1	0.045
D_{10} (mm)	0.071	0.07	0.0031	0.018
C_u	3.099	3	6.452	8.889
C_d	1.082	0.98	1.613	0.703
USCS	SP-SM	SP	SM	SM

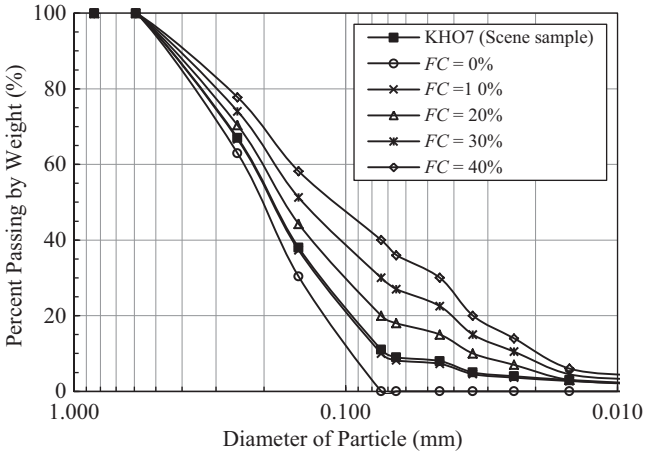

Fig. 2. Particle size distribution curves of the undisturbed and remodeled samples.

III. DIRECT SHEAR TEST

According to the ASTM-D 3080M-11 (2011) specification, samples used in a direct shear test should have a minimum diameter or width of 2″ (50 mm). The thickness should be more than 0.5″ (12.5 mm) and not less than 10 times the diameter of the largest particle size. Furthermore, the ratio of minimum diameter to thickness for cylindrical samples is 2:1. The remodeled cylindrical samples prepared for a direct shear test in this study were 120 mm in diameter and 60 mm in height.

The instruments used in this study were a traditional direct shear test apparatus affiliated with the concept of covering the sample with a rubber membrane. The configuration of the modified direct shear test apparatus is shown in Fig. 3. The main components are an air cylinder (for axial loading), screw

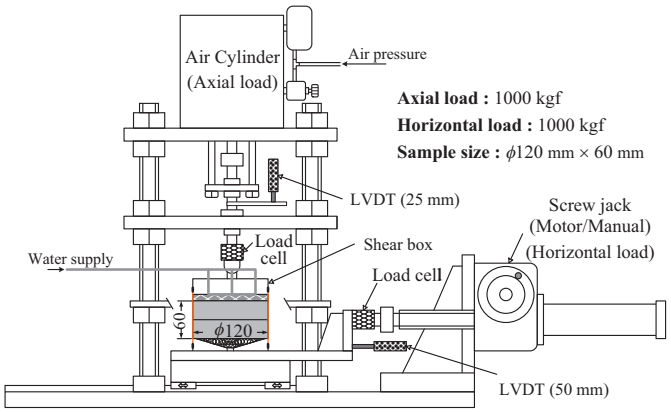

Fig. 3. Configuration of the modified direct shear test apparatus.

jack (for horizontal loading), load cells (one for each horizontal and vertical direction, with an allowable pressure of 1000 kgf), displacement gages (50 mm for the horizontal direction and 25 mm for the vertical direction), piezometers (with an allowable stress of 200 kgf/cm^2), and volume change measurement tubes.

In the traditional direct shear test, the actual volume change of the sample and increment of the excess pore water pressure were not measured directly during the shearing process. However, the volume change can be estimated from the vertical displacement measured using LVDT. Therefore, the soil samples in this study were covered with a rubber membrane to enable measuring the change in their volume and pore pressure more accurately. Thus, the volume of water discharged during the drained shear process and the change in excess pore water pressure during the undrained shear process could be measured directly.

The remodeled samples used in this study were prepared according to the relative density (D_r) and fines content (FC) required for the direct shear test (i.e., D_r = 60% and FC = 0%, 20%, or 40%). Soil was evenly mixed and placed into a box in five steps to make remodeled samples with a dimension of ϕ120 mm × 60 mm. A wet tamping method (Ishihara, 1993) was used in the sample production because some of the remodeled samples had a higher fines content. A rubber membrane was used as sample boundaries, and both halves of a shear ring (Fig. 4) were placed between the upper and lower halves of the shear box. The shear rings used in this study were designed to be 1, 5, and 10 mm in thickness and could be disassembled to form a shear surface. Thus, the thickness was regarded as the shear gap in this study. The slot between the two halves of the shear ring was used for air extraction to help fit the rubber membrane on the inner wall of the shear box to facilitate the production of the remodeled samples. Moreover, a shear ring or rubber membrane was not required when the direct shear test was proceeded with a 0-mm shear gap.

The water inflow process applied during the production of samples for this study was modified from that applied in a traditional direct shear test to produce samples as saturated as

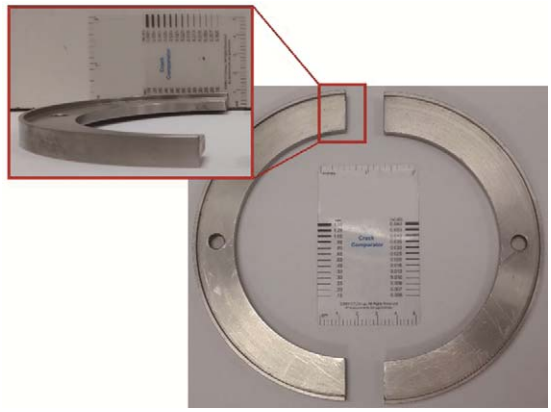

Fig. 4. Image of the shear ring (D = 5 mm).

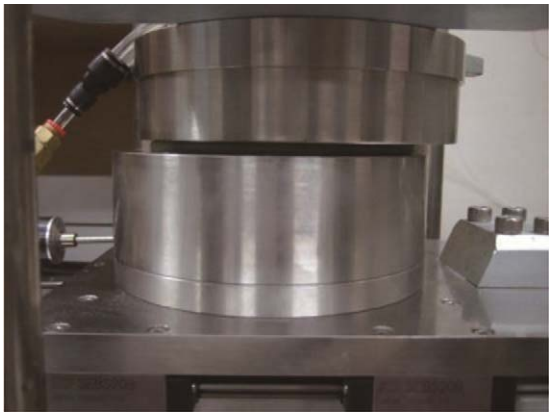

Fig. 5. Shear test process and the shear surface (D = 5 mm).

possible. Because the samples were covered with a rubber membrane, we exploited the solubility of CO_2 in the water by using it to replace the air in the pores before filling them with water. In this study, water inflow lasted approximately 30 min until it was stabilized and considered saturated.

Consolidation was performed after saturation. Different magnitudes of normal stress (σ = 500, 600, and 700 kPa) were planned, and the vertical load was adjusted using the control panel of the air cylinder. The variation in the volume change measurement tubes was measured to calculate the volume of discharged pore water to obtain the void ratio post-consolidation.

A drained shear test was conducted after the consolidation process was completed. Both halves of the shear ring had to be removed before the test to form a shear gap (Fig. 5). A quick shear (1.5 mm/min) method was used to conduct the test, and then the time required to achieve a lateral strain of 10% was calculated. The variation in the measurement tubes was recorded every 20 seconds until the test was finished. After the test was completed, the lower half of the shear box was returned to the original position. Subsequently, the sample was extracted and placed into an oven to dry before being subjected to a sieve analysis test.

Table 2. Compilation of void ratio, friction angle, and volumetric strain under different test conditions.

D (mm)	0								
FC (%)	0			20			40		
σ (kPa)	500	600	700	500	600	700	500	600	700
e	0.879	0.828	0.824	0.598	0.576	0.621	0.551	0.548	0.557
ϕ (°)	23.10	24.10	24.20	22.50	23.70	24.30	25.20	24.40	24.90
ε_v (%)	3.89	4.60	4.21	4.01	3.66	3.75	3.29	3.51	2.87
D (mm)	1								
FC (%)	0			20			40		
σ (kPa)	500	600	700	500	600	700	500	600	700
e	0.885	0.877	0.857	0.674	0.628	0.684	0.575	0.584	0.589
ϕ (°)	23.90	26.10	25.80	25.90	28.00	28.20	25.80	27.20	28.10
ε_v (%)	3.38	3.62	4.15	3.13	3.98	3.09	2.76	2.91	2.80
D (mm)	5								
FC (%)	0			20			40		
σ (kPa)	500	600	700	500	600	700	500	600	700
e	0.898	0.898	0.893	0.678	0.651	0.662	0.621	0.611	0.602
ϕ (°)	21.80	23.80	24.40	20.60	22.60	23.40	23.30	24.70	26.10
ε_v (%)	3.35	3.38	3.69	2.85	3.63	3.09	2.40	3.16	3.10
D (mm)	10								
FC (%)	0			20			40		
σ (kPa)	500	600	700	500	600	700	500	600	700
e	0.950	0.922	0.920	0.710	0.740	0.687	0.654	0.643	0.713
ϕ (°)	23.50	20.40	24.30	21.50	23.70	23.80	23.20	22.90	22.30
ε_v (%)	2.53	2.51	2.98	2.66	2.80	2.92	2.15	2.29	2.02

IV. RESULTS AND ANALYSIS

In this study, the remodeled samples composed of KHO7 with a relative density of 60% were tested under various test conditions. As described, the settings of the test were the shear gap (0, 1, 5, and 10 mm), fines content (0%, 20%, and 40%), and normal stress (500, 600, and 700 kPa). The void ratio after consolidation (e), friction angle (ϕ), and volumetric strain (ε_v) obtained under different test conditions are presented in Table 2.

The test results for the remodeled sample with a 0% fines content showed that its void ratio after consolidation was between 0.82 and 0.95. The test results for the remodeled sample with a 20% to 40% fines content showed that its void ratio after consolidation was between 0.55 and 0.74. Although still influenced by the FC and shear gap, no obvious relationship between the void ratio and volumetric strain was observed.

Fig. 6 shows the relationship between the shear gap and friction angle. The squares, circles, and triangles in the figure represent a fines content of 0%, 20%, and 40%, respectively. The filled, unfilled, and diagonally hatched shapes represent the normal stresses of 500, 600, and 700 kPa, respectively. The results revealed that the friction angles were between 20° and 28° and that the value increased as the normal stress increased. Furthermore, for all the samples tested under various conditions, the friction angle was consistently the highest

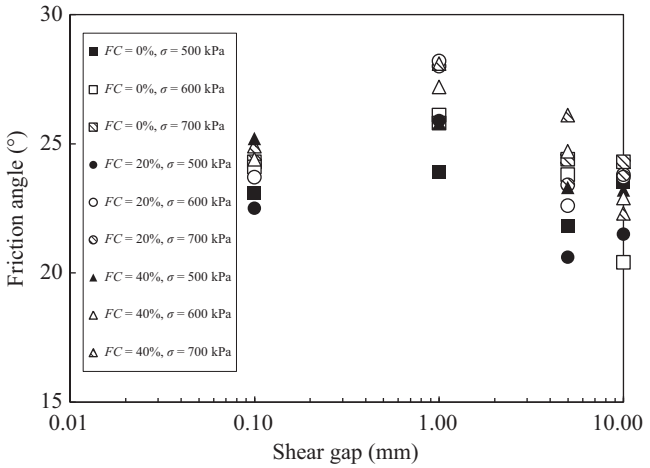

Fig. 6. Relationship between shear gap and friction angle.

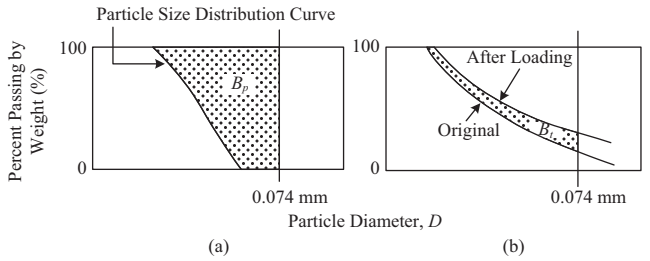

Fig. 7. Schematic diagram of Breakage Potential and Total Breakage (Hardin, 1985).

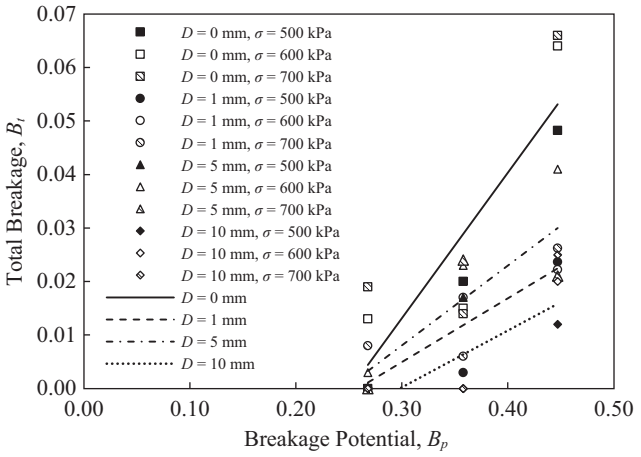

Fig. 8. Relationship between breakage potential and total breakage at various shear gaps.

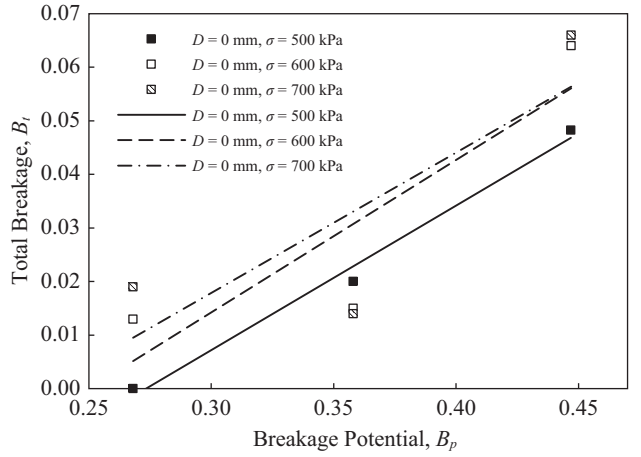

Fig. 9. Relationship between breakage potential and total breakage (D = 0 mm).

when the shear gap was 1 mm. This result might have been caused by the influence of the stiffness of the rubber membrane covering the samples on the soil strength when the shear gap was insufficient.

1. The Calculation and Analysis of B_p, B_t and B_r

The aforementioned breakage potential (B_p) and total breakage (B_t) proposed by Hardin (1985) was used as the basis of analysis in this study. The breakage potential (B_p) was represented as the area between the line particle size D = 0.0744 mm and the part of the particle size distribution curve for which D was larger than 0.074 mm. The value of B_p was calculated using the integration process for each sieve size, as shown in Fig. 7(a). B_t represents the total breakage, which was equal to the original breakage potential minus the breakage potential after loading. To obtain the value of B_t, the area of the region between grain size distribution lines before and after the loading (Fig. 7(b)) was also calculated using the integration process. The relationship between the breakage potential and total breakage at various shear gaps is shown in Fig. 8. The squares, circles, triangles, and diamonds in the figure represent shear gaps of 0, 1, 5, and 10 mm, respectively. The filled, unfilled, and diagonally hatched shapes represent the normal stresses of 500, 600, and 700 kPa, respectively. The solid, dashed, dash-dotted, and dotted lines represent the relationship tendency between B_p and B_t when the shear gap was 0, 1, 5, and 10 mm, respectively. A large shear gap means that the soil particles are more likely to produce overstepping behavior, which could cause a low total breakage (B_t) after shearing. Therefore, if the breaking potential is unchanged, increasing the shear gap decreases the relative breakage ($B_r = B_t/B_p$). Furthermore, the relationship between the breakage potential and total breakage when the shear gap was 0 mm is shown in Fig. 9. The definitions of the symbols in this figure are the same as those mentioned in Fig. 8. The results revealed that increasing the normal stress increased the total breakage, and increasing the breakage potential also increased the total breakage.

2. The Influences of the Void Ratio, Fine Particles, and Increment of Fines Content

The relationship between the total breakage and FC is shown in Fig. 10. The definitions of the symbols in this figure

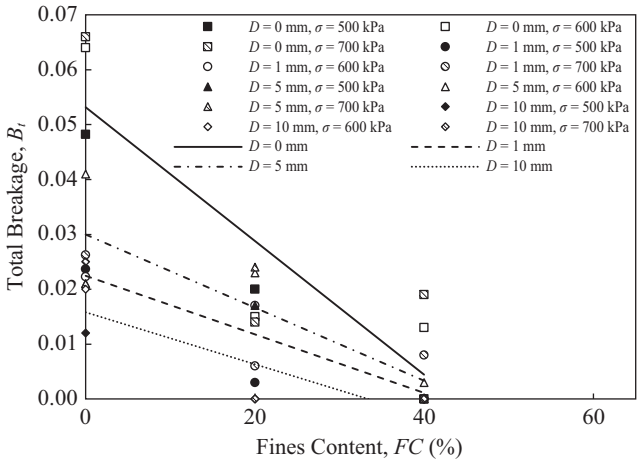

Fig. 10. Relationship between total breakage and fines content.

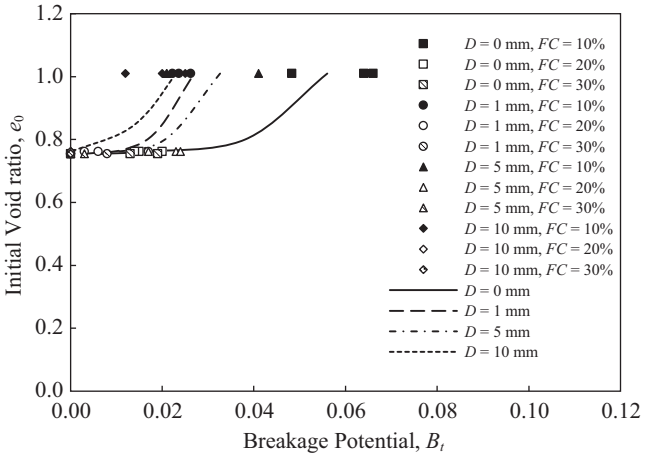

Fig. 12. Relationship between initial void ratio and total breakage.

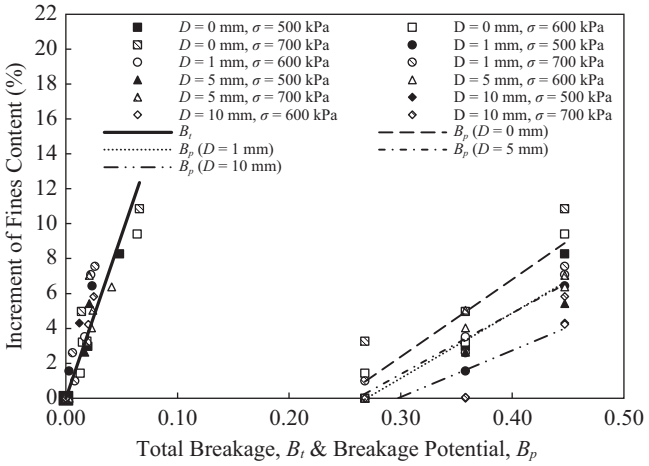

Fig. 11. Relationship between total breakage, breakage potential, and increment of fines content.

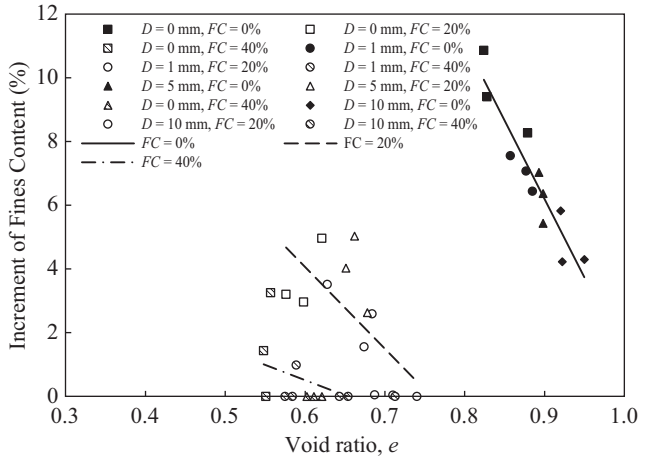

Fig. 13. Relationship between void ratio and increment of fines content.

are the same as those mentioned in Fig. 8. The lines represent the relationship tendency between the total breakage and *FC* at different shear gaps. The results indicated that a high fines content and large shear gap caused a low total breakage during the shearing process because the finer particles filling the void increased the contact area between the particles and significantly reduced stress concentration phenomena, which eventually decreased the probability of particle breakage. In addition, a large shear gap means that the soil particles are more likely to produce overstepping behavior during the shearing process, which could lead to a low total breakage.

The relationship among the breakage potential, total breakage, and increment of *FC* after shearing is shown in Fig. 11. The symbols in this figure have the same definitions as those mentioned previously. The increment of *FC* after shearing could be determined from the difference between the percentage of *FC* after shearing and the percentage of *FC* during the production of the remodeled samples. The results showed a positive relationship between the total breakage and increment of *FC* after shearing, whereas an increasing breaking potential increased the increment of *FC* after shearing regardless of the shear gap.

Hardin (1985) assessed and defined the breakage potential according to the initial void ratio (e_o) of remodeled samples under various test conditions. The relationship between the initial void ratio and total breakage is shown in Fig. 12, in which the total breakage is represented by the *x*-axis and the initial void ratio is represented by the *y*-axis. The definitions of the symbols are the same as those described previously. The test results indicated that the void ratio was influenced by *FC* regardless of the shear gap. The initial void ratio for samples with an *FC* of 20% and 40% were markedly similar, with values ranging between 0.75 and 0.76. However, when the fines content was 0%, the initial void ratio was approximately 1.0. The test results showed that a small shear gap lead to a high total breakage.

The relationship between the void ratio after consolidation and the increment of *FC* after shearing is shown in Fig. 13. The squares, circles, triangles, and diamonds in the figure

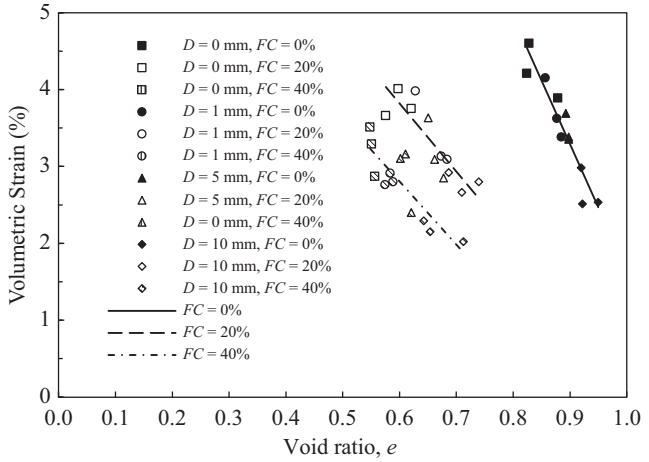

Fig. 14. Relationship between void ratio and volumetric strain.

represent shear gaps of 0, 1, 5, and 10 mm, respectively. The filled, unfilled, and diagonally hatched shapes represent the fines content of 10%, 20%, and 40%, respectively. The results were clearly classified into three types that show the influence of *FC* on the soil. A high fines content lead to a small increment of *FC*. When the fines content was unchanged, a large shear gap yielded a high void ratio and a small increment of *FC* after shearing.

The relationship between void ratio and volumetric strain after consolidation is shown in Fig. 14. The definitions of the symbols in this figure are the same as those mentioned in Fig. 13. Similar to those shown in Fig. 13, the results were also clearly classified into three types that indicated the influence of *FC* on the soil. A high fines content lead to a low volumetric strain. In Fig. 14, for samples with the same fines content, the large shear gap caused a higher tendency of a void ratio and a low tendency of volumetric strain.

V. CONCLUSION

A modified direct shear test apparatus was used in this study to simulate and examine the breakage characteristics of fine soil particles through a series of tests conducted on remodeled samples of Kaohsiung sand with various shear gaps, normal stresses, and fines content. The results of this study are as follows:

1. A large normal stress and a high breakage potential lead to a high total breakage. In addition, a large shear gap means that the soil particles are more likely to produce overstepping behavior, which could cause a low total breakage during the shearing process. Therefore, if the breaking potential is unchanged, an increasing shear gap decreases the relative breakage ($B_r = B_t/B_p$).
2. The contact area between particles is increased as the void between larger particles is filled by finer particles, which could significantly reduce the stress concentration phenomena. Furthermore, a large shear gap means that the soil particles are more likely to produce overstepping behavior during the shearing process. Therefore, a high fines content and large shear gap cause a low total breakage during the shearing process.
3. A high breakage potential leads to a large increment of *FC* after shearing regardless of the shear gap, and a positive relationship between the total breakage and increment of *FC* is observed after shearing.
4. Soil is influenced by its fines content. A high fines content in the soil causes a small increment of *FC* and low volumetric strain after shearing. When the fines content is unchanged, an increasing shear gap increases the void ratio and decreases the increment of *FC* after shearing as well as its volumetric strain.

ACKNOWLEDGMENTS

The authors would like to thank Prof. Kenji Ishihara, Prof. Takaji Kokusyo (CHUO University, Tokyo, Japan), and Prof. Yie-Ruey Chen (Chang Jung Christian University, Tainan, Taiwan) for their help and advice during instrument development and design and suggestions for the procedures of the test.

REFERENCES

ASTM D3080M-11 (2011). Standard test method for direct shear test of soils under consolidated drained conditions. ASTM International, West Conshohocken, PA.

Hardin, B. O. (1985). Crushing of soil particles. Journal of the Geotechnical Engineering Division. ASCE 3(10), 1177-1192.

Ishihara, K. (1993). Liquefaction and flow failure during earthquake. Geotechnique 43(3), 315-415.

Lee, K. L. and I. Farhoomand (1967). Compressibility and crushing of granular soil in anisotropic triaxial compression. Canadian Geotechnical Journal 4(1), 68-86.

Lee, K. L. and H. B. Seed (1967). Drained strength characteristics of sands. Journal of the Soil Mechanics and Foundations Division, ASCE 93 (SM6), 117-141.

Lee, W. F., K. Ishihara, C. C. Chen, J. W. Chen and M. H. Chang (2012). Study on the engineering properties of non-plastic silty sand in Taiwan. Sino-Geotechnics 133, 7-18.

Leslie, D. D. (1963). Large scale triaxial tests on gravelly soils. Proceedings of the 2nd Panamerican Conference on Soil Mechanics and Foundation Engineering, Brazil 1, 181-202.

Leslie, D. D. (1975). Shear strength of rockfill. Physical Properties Engineering Study No. 526, South Pacific Division, Corps of Engineers Laboratory, Sausalito, Calif., Oct., 124.

Marsal, R. J. (1965). Discussion of shear strength. Proceedings of the 6th International Conference on Soil Mechanics and Foundation Engineering, Montreal 3, 310-316.

Miura, N., H. Murata and A. Harada (1983). Effect of water on the shear characteristics of sandy soils consisted of breakable particles. Transactions of the Japanese Society of Civil Engineering 15, 377-380.

Zhang, J. M., G. S. Jiang and R. Wang (2009). Research on influences of particle breakage and dilatancy on shear strength of calcareous sands. Rock and Soil Mechanics 30(7), Jul., 2043-2048.

Zhao, G. S., G. Q. Zhou, F. P. Zhu and X. Y. Bie (2008). Experimental research on the influence of particle crushing on direct shear strength of sand. Journal of China University of Mining & Technology 37(3), 291-294.